



HAL
open science

van der Waals forces stabilize low-energy polymorphism in B₂O₃: Implications for the crystallization anomaly

Guillaume Ferlat, Maria Hellgren, François-Xavier Coudert, Henri Hay, Francesco Mauri, Michele Casula

► To cite this version:

Guillaume Ferlat, Maria Hellgren, François-Xavier Coudert, Henri Hay, Francesco Mauri, et al.. van der Waals forces stabilize low-energy polymorphism in B₂O₃: Implications for the crystallization anomaly. *Physical Review Materials*, 2019, 3 (6), pp.063603. 10.1103/PhysRevMaterials.3.063603 . hal-02152193

HAL Id: hal-02152193

<https://hal.science/hal-02152193>

Submitted on 11 Jun 2019

HAL is a multi-disciplinary open access archive for the deposit and dissemination of scientific research documents, whether they are published or not. The documents may come from teaching and research institutions in France or abroad, or from public or private research centers.

L'archive ouverte pluridisciplinaire **HAL**, est destinée au dépôt et à la diffusion de documents scientifiques de niveau recherche, publiés ou non, émanant des établissements d'enseignement et de recherche français ou étrangers, des laboratoires publics ou privés.

van der Waals forces stabilize low-energy polymorphism in B_2O_3 : implications for the *crystallization anomaly*

Guillaume Ferlat,¹ Maria Hellgren,¹ François-Xavier Coudert,² Henri Hay,¹ Francesco Mauri,^{1,3} Michele Casula¹

¹*Sorbonne Université, MNHN, UMR CNRS 7590, IRD, IMPMC, F-75005 Paris, France*

²*Chimie ParisTech, PSL University, CNRS, Institut de Recherche de Chimie Paris, 75005 Paris, France*

³*Dipartimento di Fisica, Università di Roma La Sapienza, Piazzale Aldo Moro 5, I-00185 Roma, Italy*

(Dated: May 15, 2019)

The cohesive energies and structural properties of recently predicted - and never synthesized - B_2O_3 polymorphs are investigated from *first-principles* using density functional theory and high-accuracy many-body methods, namely the random phase approximation and quantum Monte Carlo. We demonstrate that the van der Waals forces play a key role in making the experimentally known polymorph (B_2O_3 -I) the lowest in energy, with many competing metastable structures lying only a few kcal/mol above. Remarkably, all metastable crystals are comparable in energy and density to the glass, while having anisotropic and mechanically soft structures. Furthermore, the best metastable polymorph according to our stability criteria has a structural motif found in both the glass and a recently synthesized borosulfate compound. Our findings provide new perspectives for the understanding of the B_2O_3 anomalous behavior, namely its propensity to vitrify in a glassy structure drastically different from the known crystal.

I. INTRODUCTION

Diboron trioxide (B_2O_3) not only is the second most used component of industrial glasses after silica (SiO_2), but also a canonical network-forming system *per se* (see e.g. Refs. [1, 2] for reviews). The originality of the low-pressure B_2O_3 networks, either crystalline or vitreous, stems from their building blocks, which are bi-dimensional (2D) trigonal (BO_3) units. This is in contrast with most network-formers, such as silica, based on three-dimensional (3D) tetrahedral units. Fully 3D networks are then formed by binding these rigid units through flexible cation-oxygen-cation bonds, which give B_2O_3 low-density structures, and a great potential for polymorphic transformations, under e.g. high-temperature or pressure. This is clearly reflected by various studies showing polyamorphic transformations in the glass [3–7] and to a lesser extent in the liquid [8, 9].

However, our knowledge of the B_2O_3 crystalline forms remains very limited: up to now, only one low-pressure BO_3 -based crystal (B_2O_3 -I) has been experimentally characterized [10] in addition to a high-pressure phase (B_2O_3 -II), based upon BO_4 tetrahedral units. The possible existence of another low-density polymorph - of unidentified structure - has been reported long ago [11], but the status of this report remains unclear since subsequent attempts failed to reproduce it. This is in sharp contrast with the rich polymorphism found in other oxide systems: in silica [12], for instance, more than 20 low-pressure polymorphs (from coesite to zeolites) built upon the same basic units have been experimentally reported.

Another striking and very uncommon feature is the *abnormal structural dissimilarity* between the glassy (g- B_2O_3) and crystalline forms. In g- B_2O_3 , about half of the BO_3 elemental bricks are arranged into superstructural units, i.e. three-fold rings referred to as boroxol rings [13, 14], fully absent from B_2O_3 -I (see Fig. 1). As a

consequence, the glass density is considerably smaller ($\sim -30\%$) than the B_2O_3 -I one. Likely related [15] but yet not understood, is the extremely high glass-forming ability of B_2O_3 , arguably the best glass former. Indeed, the B_2O_3 -I crystallization has never been observed from ambient pressure liquid, even if seeded with germs for months. The synthesis requires cooling the liquid under pressure, or alternatively using chemical routes, a behavior which has been coined as the *crystallization anomaly* [16].

Mostly inspired by the structural differences between g- B_2O_3 and B_2O_3 -I, several theoretical works have predicted additional polymorphs [17–20]. In particular, a set of 25 new crystals [19], further complemented by two additional ones [20], has recently been obtained using density functional theory (DFT). It spans a very narrow energy range (a few kcal/mol), with values comparable to, or even lower than, B_2O_3 -I, therefore challenging it as the ground state. Hence, high-level theories are needed to go beyond the standard approximations (LDA, GGA) that have been used in all previous DFT works. As a matter of fact, a drastically different physical picture emerges from our high-level calculations as it will be shown later.

In the current work, we employ accurate many-body methods such as quantum Monte Carlo (QMC) and the random phase approximation (RPA) to provide a definitive answer to the relative stability between B_2O_3 -I and a subset of predicted polymorphs. In addition, we present results for a large set of polymorphs at different levels of DFT which demonstrate a huge effect of the van der Waals (vdW) forces on both the structures and energetics, an effect that has been neglected in all previous studies [17–20]. We definitely assess B_2O_3 -I as the ground state while we introduce a new polymorph (T0-0.5b), adapted from a recently synthesized borosulfate structure [21] which we reveal as the most stable among all putative structures. Its layers are decorated by triangle and boroxol units (Fig. 1) in equal proportions (1:1), making it a close - albeit crystalline - structural approximant of the glass.

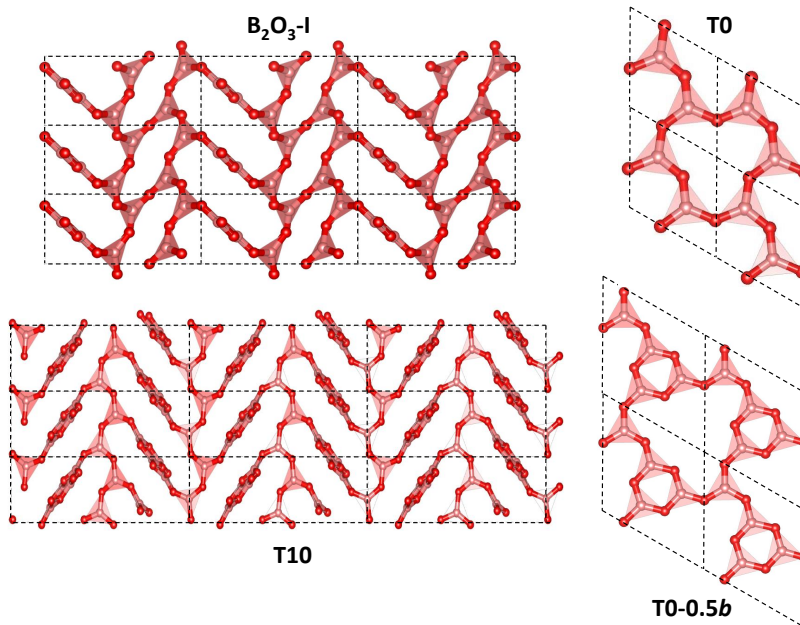


Figure 1. Left: $3 \times 3 \times 3$ supercell of B_2O_3 -I and T10 seen in the (a, c) plane. Right: layers of T0 and T0-0.5b, the latter based on a mixed decoration of BO_3 triangle and boroxol units. All the polymorphs considered in this work are 3D-networks with the exception of T0, T0-0.5b, and T0-*b* which are layered structures.

II. METHODS

Highly accurate QMC simulations have been carried out on 3 polymorphs (B_2O_3 -I and two predictions T0 and T10). We used a Jastrow-Slater variational wave function, with Slater and Jastrow parts developed on a localized Gaussian basis set. The Jastrow factor contains correlation terms up to the 4-body (electron-ion-electron-ion) form, able to capture van der Waals effects within variational Monte Carlo (VMC) [22]. The wave function has been fully optimized (Slater orbitals together with Jastrow coefficients) by energy minimization [23], starting from DFT-LDA generated 1-body orbitals. Moreover, we have performed a complete structural relaxation for both cell parameters and internal coordinates at the VMC level [24]. Then, using relaxed VMC geometries, we have carried out lattice-regularized diffusion Monte Carlo simulations [25, 26] and a very accurate finite-size extrapolation [27] in order to provide energies with accuracy better than 1.0 kcal/mol. A careful convergence of all relevant criteria, i.e. basis set, geometry, finite-size effects and level of theory, is necessary, given the phase-space proximity of the B_2O_3 polymorphs. All QMC calculations have been performed using the TurboRVB code [28]. Further details can be found in the Supporting Material (SM) [29].

Calculations with the RPA were performed on a larger set of 6 polymorphs (B_2O_3 -I, T0, T10, T3, T0-0.5b and T0-*b*). The RPA is a state-of-the-art density functional approach based on many-body perturbation theory and the adiabatic connection fluctuation-dissipation formula [30, 31]. By including polarization diagrams to

infinite order in the Coulomb interaction the RPA captures vdW forces [32, 33]. It also provides an accurate description of Hartree-Fock exchange, and an overall good description of correlation effects (at least as long as energy differences are concerned). RPA total energies were calculated with the VASP code [34, 35]. Computational details can be found in the SM [29].

Dispersive interactions can also be added in a semi-empirical form to standard DFT approximations such as in the DFT-D approaches: for instance, in D2 [36] the vdW interactions coefficients (C_6) are fixed for a given atomic pair while in the TS approach [37], they are calculated self-consistently according to the atomic neighborhood. At a more advanced level, vdW are accounted for in fully non-local functionals that include polarization effects from first-principles, such as in the vdW-DFT class of functionals [38, 39]. In this work, we used representative functionals from these different levels, namely D2 [36], TS [37] (added on top of the PBE functional [40], using the CASTEP code [41]) and the recently derived DF-cx [39] vdW-DFT functional (using the Quantum Espresso package [42]). We checked explicitly that the use of different codes and pseudo-potentials does not affect the reported results (Fig. S1 of the SM [29]). We also report results from LDA and GGA (PBE) functionals as references. In particular, the comparison between GGA and dispersion-corrected schemes (D2 and TS) built upon the same GGA, allows one to probe straightforwardly the relevance of vdW interactions. Thanks to the low computational cost of DFT, we studied a total of 27 polymorphs (those from Ref. [19] supplemented with T0-0.5b), which contain up to 135 atoms per unit cell [19].

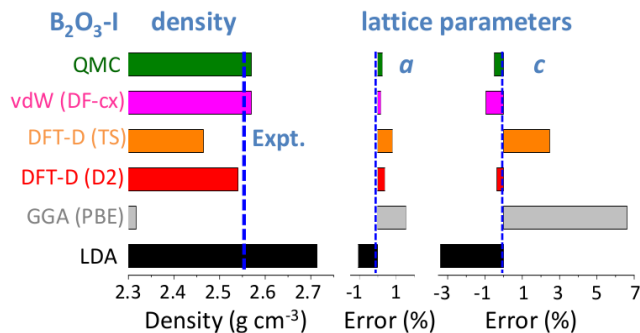


Figure 2. Density and lattice parameters of B_2O_3 -I from different *ab initio* schemes. Errors on lattice parameters are expressed relatively to the experimental values.

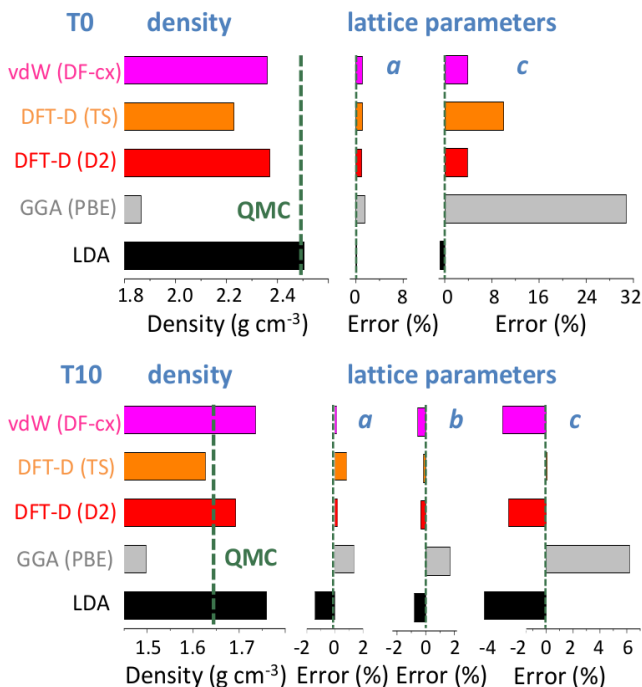


Figure 3. Density and lattice parameters of T0 and T10 from different *ab initio* schemes. Errors on lattice parameters are expressed relatively to the QMC values.

Finally, we studied the mechanical properties via DFT-D2 calculations of second-order elastic constant tensors following a methodology described elsewhere [43, 44]. See the SM for all the details of the DFT calculations [29].

III. RESULTS AND DISCUSSION

We first assess the quality of the structural results obtained from the different schemes by relaxing the B_2O_3 -I structure, and taking the experimentally known geometry as reference (Fig. 2). Not surprisingly, the lattice parameters obtained with LDA are underestimated (and

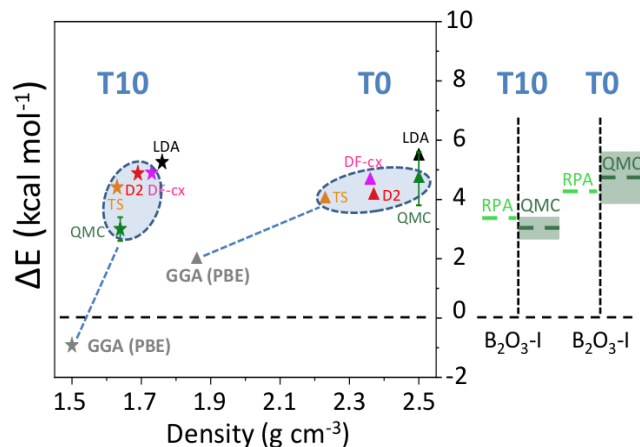


Figure 4. Left: energies, relative to B_2O_3 -I, from the different schemes for two predicted polymorphs, T0 (triangles) and T10 (stars). The blue shaded ellipses encompass vdW-corrected results. Right: RPA and QMC energies compared. The green shaded rectangles correspond to the QMC error bars.

the density overestimated by +6 %) while the opposite is true for PBE (density error of -10 %). This reflects the well-documented tendencies [45, 46] of LDA to overbind and of PBE to underbind. Note, however, that the size of these errors is large for a non-layered inorganic system, placing B_2O_3 -I in the topmost range (95th percentile) of volume errors for inorganic materials of the Materials Project database [47]. Interestingly, these deficiencies are largely cured not only by QMC (+0.5 % error on density) but also by all the vdW-corrected schemes used here, which show a systematic improvement.

Although B_2O_3 -I is a fully connected 3D-network made of strong interatomic bonds, the importance of the vdW corrections stems from the structural porosity, arising from *locally planar* regions - on the scale of a few building units - arranged in a *zig-zag* pattern thanks to the B-O-B angular flexibility (Fig. 1). This leads to a *softer* direction, perpendicular to the locally planar regions, and nearly parallel to the *c* direction, as reflected by larger errors in this lattice parameter (Fig. 2). The existence of such a softer direction is found in all but two polymorphs (see also Fig. 3).

We now focus on the densities and energies of two previously predicted [19] polymorphs, namely T0 and T10 using QMC results as reference in the absence of experimental data. We report these results in Figs. 3 and 4. In the following, all crystals' energies are expressed with respect to the B_2O_3 -I one. Similarly to the experimentally known case, PBE severely underestimates the densities. This impacts the energies, which are also underestimated. Note that T10, which in the PBE original predictions [19] had a slightly lower energy (~ -1 kcal/mol) than B_2O_3 -I, turns out to be metastable ($\sim +3$ kcal/mol). On the contrary, the vdW-corrected DFT schemes perform reasonably well in both densities and energies. Moreover, the RPA energies agree well with QMC (Fig. 4, right panel).

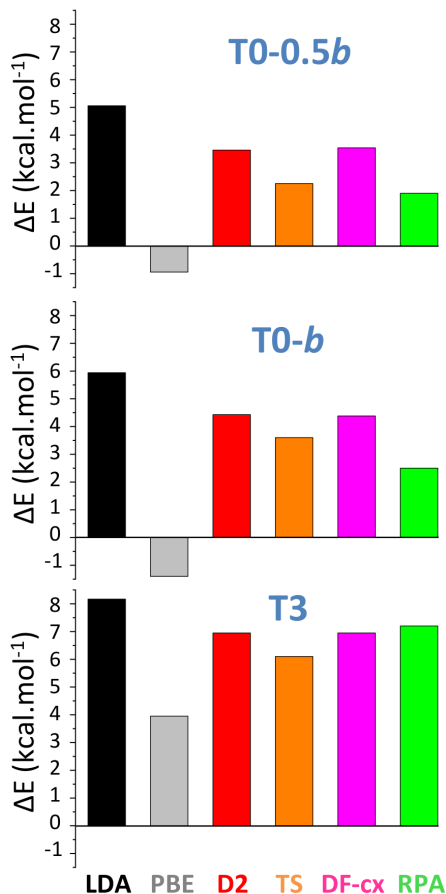


Figure 5. Energies, relative to B_2O_3 -I (in kcal mol^{-1}) obtained from the different *ab initio* schemes, including RPA, for three polymorphs (T0-0.5b, T0-b, T3). The energies for T0 and T10 are reported in Fig. 4.

We also calculated RPA energies for the T0-0.5b, T0-b, and T3 structures, shown in Fig. 5 together with those from the different DFT schemes. We note that all three vdW-corrected functionals yield essentially the same results, with a typical variability of 2 kcal/mol on the energies, and compare well with the more advanced RPA. This gives strong confidence in the overall picture. A complete account for the full set of 27 B_2O_3 polymorphs, using the various DFT frameworks, is reported (Fig. S2) in the SM [29]. In the following we shall take D2 as representative of the vdW-corrected functionals [48], in order to make a thorough comparison with PBE, and show the impact of the dispersive interactions on the B_2O_3 polymorphism.

Fig. 6 highlights the density and energy corrections brought back by the vdW contributions. Being attractive, the vdW forces systematically provide denser structures (Fig. 6, left panel), on average by 40 % and by up to 150 % for some polymorphs, such as T8-b. Such high figures reflect the fact that for many polymorphs the vdW scheme allows one to find a qualitatively different geometry from the PBE one (e.g. internal voids and

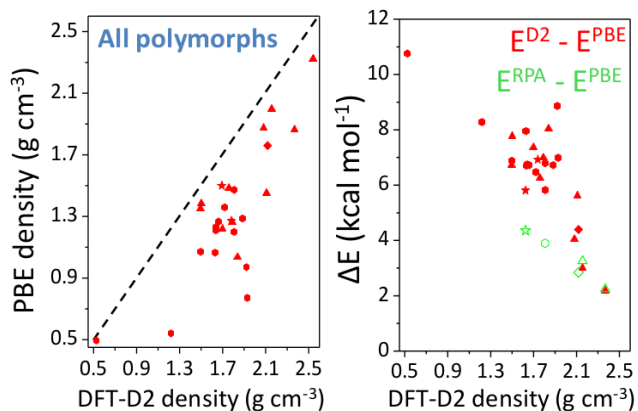


Figure 6. Corrections to the PBE density (left panel) and relative energy (right panel) brought back by the vdW-corrected schemes, using DFT-D2 (red) or RPA (green symbols).

large-scale rings tend to be less symmetric and more puckered). This densification effect, which acts effectively as an internal negative pressure, results in an increasing enthalpic penalty with decreasing density (Fig. 6, right panel). Overall, the more porous the polymorph, the larger the vdW contribution to the energy. This trend is supported by the RPA results presented in the same figure, and is also in line with studies of e.g. silica zeolites [46]. In other words, the energies of the predicted polymorphs are more impacted by vdW than the B_2O_3 -I one, because of their lower density.

The energy diagram (Fig. 7, left panel) resulting from the vdW inclusion provides several major outcomes. First, all predicted polymorphs energies fall above B_2O_3 -I, while in the PBE picture [19, 20] many polymorphs are possible candidates for the ground state. Note that the overall correlation between metastability and density is now in line with the one observed for silica polymorphs [43]. Although the results are presented at 0 K, we checked that the picture obtained at 300 K is unchanged within 1 kcal/mol (by computing finite-temperature contributions to the vibrational free-energy within the DFT-D2 scheme, see the SM [29]). A second important point is that, despite being metastable, most of the predicted polymorphs are still within a thermodynamically accessible energy range, estimated at ~ 7 kcal/mol [49]. In particular, polymorphs such as T0-0.5b and T0-b could be amenable to synthesis. Remarkably, the layers that constitute these polymorphs are found experimentally in several chemically-complex borates [21, 50, 51].

However, assessing the synthesizability of a given polymorph is a very challenging task, since the energy is not the sole ingredient at play. Following an earlier work on silica zeolites which associated experimentally observed structures with good mechanical properties [43], we undertook a comprehensive characterization of the mechanical properties of the B_2O_3 polymorphs, including bulk (B), Young (E) and shear (G) moduli as well as linear compressibility and Poisson's ratio [44]. In all the calculated

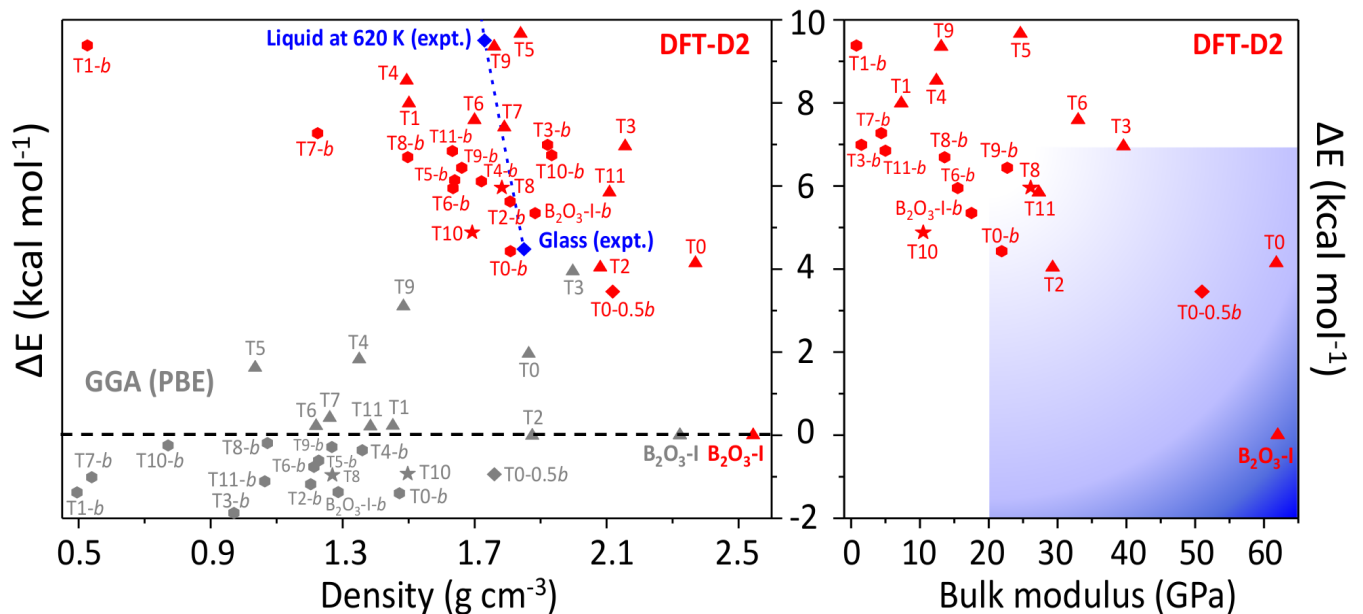


Figure 7. Left: Energy, relative to B₂O₃-I, and density for all polymorphs using DFT-D2 (red) and PBE (grey symbols). Symbols refer to the relative proportions of structural units (triangles:boroxol) in the polymorphs: \triangle only BO₃ triangles (1:0), \circ only boroxol rings (0:1), \star mixed decoration (3:1), \diamond mixed decoration (1:1). Experimental data (liquid and glass) are from Ref. [52]. Right: energy and bulk modulus using DFT-D2. The inner rectangle schematically represents the *feasibility* window.

moduli, and as illustrated in Fig. 7 (right panel) for the bulk modulus, there is a rather clear distinction between B₂O₃-I ($B \sim 60$ GPa) and most of the other polymorphs which show much smaller values (~ 0 -30 GPa). For illustrative purposes, the shaded-blue rectangle in the energy-versus- B parameter space delimits the ranges of values in experimentally-realized silica polymorphs. Noticeably, this area excludes most of the predicted B₂O₃ polymorphs, with a few noticeable exceptions including T0- b and T0-0.5 b .

Further, for most polymorphs, E and G - which are directional quantities - show high anisotropies, implying that there is one direction much *weaker* than the others with respect to an applied stress. This is in line with the aforementioned *soft* direction in these structures. In silica zeolites [43], proposals of *feasibility* criteria were derived from the lowest values of these mechanical quantities: strictly transferring these criteria [53] to B₂O₃ leaves only B₂O₃-I as a realizable structure with however a handful of additional candidates (T3, T11, B₂O₃-I- b , T0, T0-0.5 b) close to the criteria thresholds. Thus, many of the predicted structures suffer from mechanical stability issues and this may be one of the reasons why they have not been experimentally realized yet.

Our findings have strong implications for understanding the B₂O₃ behavior at the glass transition. Indeed, the vast majority of the predicted polymorphs are clustered close to the liquid and glass states in the energy-density diagram (dashed-blue line in Fig. 7, left panel). Since the glass structure is generally expected to resemble that of the underlying crystals, Fig. 7 provides a framework to

understand the glass state and its apparent anomalous properties, such as its low density, its high fraction of rings, and its strong structural dissimilarity with B₂O₃-I. In addition, the existence of many competing polymorphs of similar energies, as observed here, has been shown to correlate with the glass forming ability; a situation reported for a large range of systems [54, 55] and in various models [56–58].

These aspects, which combine the energetics with the mechanical properties, allow one to propose the following explanation for the B₂O₃ *crystallization anomaly*. As the low-density liquid is cooled and gets closer to the region of high polymorphic degeneracy, it hovers over a rugged energy landscape, i.e. dominated by many local minima of similar energies. These minima are associated to low-density and mechanically-weak structures prone to collapse into an amorphous framework. Although there exists a ground state (B₂O₃-I) of higher density, the driving force (energy separation between the metastable states and B₂O₃-I) is small enough and the energy barriers (associated to the topological reconfiguration required to reach the B₂O₃-I density) are sufficiently high so that the system is kinetically trapped, in accordance with the very sluggish kinetics found in this system [15]. Applying pressure to the melt favors higher density and stiffer structures in the energy landscape, and thus results in the B₂O₃-I crystallization.

IV. CONCLUSIONS

We have revealed that B_2O_3 is a system remarkably sensitive to vdW interactions in both energies and structures. The importance of vdW in B_2O_3 is striking and unexpected, particularly when compared to SiO_2 , a system commonly considered similar for which however only mild effects from vdW have been reported [46]. Thus, the set of polymorphs studied in this work constitutes a valuable test-bed to develop new methods for the accurate treatment of electronic correlation. At the same time, the account of vdW allows to retrieve a polymorphic picture which not only supports the generally admitted experimental knowledge (B_2O_3 -I is the ground-state) but also brings the metastable polymorphs closer to the glass in the energy-density phase-space. From the simultaneous characterization of energies and mechanical properties carried out here, we provide a semi-quantitative map of the *likeliness of synthesizability*. Not only is it in agreement with the experimental observations - the structural

motif from the most robust predicted polymorph (T0-0.5b) has been found in synthesized borates - but also it provides a fundamental framework to explain the B_2O_3 intriguing anomalies. The glass has a low density and a high amount of boroxol rings because the supercooled liquid acquires those structural characteristics from the closest underlying crystalline polymorphs. It however fails to crystallize in any of these because of their weak mechanical properties.

ACKNOWLEDGMENT

We thank H. Hillebrecht for communicating the results of Ref. [21] prior to their publication. This work was performed using HPC resources from GENCI-TGCC/CINES/IDRIS (Grants A0030906493, A0030801875, A0010906493 and A0010907625) and from PRACE (project 2016143322). Financial supports from the French National Research Agency program PIPOG ANR-17-CE30-000 and from the program Emergence-Ville de Paris are acknowledged.

-
- [1] G. Ferlat, *Rings in Network Glasses: The B_2O_3 Case* (Springer, Switzerland, 2015), chap. 14, p. 367.
- [2] A. C. Wright, Phys. Chem. Glasses: Eur. J. Glass Sci. Technol. B **59**, 65 (2018).
- [3] J. Nicholas, S. Sinogeikin, J. Kieffer, and J. Bass, Phys. Rev. Lett. **92**, 215701 (2004).
- [4] S. K. Lee, K. Mibe, Y. Fei, G. D. Cody, and B. O. Mysen, Phys. Rev. Lett. **94**, 165507 (2005).
- [5] K. Trachenko, V. V. Brazhkin, G. Ferlat, M. T. Dove, and E. Artacho, Phys. Rev. B **78**, 172102 (2008).
- [6] A. Zeidler, K. Wezka, D. A. J. Whittaker, S. P. Salmon, A. Baroni, S. Klotz, H. E. Fischer, M. C. Wilding, C. L. Bull, M. G. Tucker, et al., Phys. Rev. B **90**, 024206 (2014).
- [7] S. K. Lee, Y.-H. Kim, P. Chow, Y. Xiao, J. Cheng, and G. Shen, Proc. Natl. Acad. Sci. USA **115**, 5855 (2018).
- [8] V. V. Brazhkin, I. Farnan, K. I. Funakoshi, M. Kanzaki, Y. Katayama, A. G. Lyapin, and H. Saitoh, Phys. Rev. Lett. **105**, 115701 (2010).
- [9] O. L. G. Alderman, G. Ferlat, A. Baroni, M. Salanne, M. Micoulaut, C. J. Benmore, A. Lin, A. Tamaloni, and J. K. R. Weber, J. Phys. Condens. Matter **27**, 455104 (2015).
- [10] G. E. Gurr, P. W. Montgomery, C. D. Knutson, and B. T. Gorres, Acta Crystallogr. **B26**, 906 (1970).
- [11] S. S. Cole and N. W. Taylor, J. Am. Ceram. Soc. **18**, 55 (1935).
- [12] P. M. Piccione, C. Laberty, S. Yang, M. A. Camblor, A. Navrotsky, and M. E. Davis, J. Phys. Chem. B **104**, 10001 (2000).
- [13] R. E. Youngman, S. T. Haubrich, J. W. Zwanziger, M. T. Janicke, and B. F. Chmelka, Science **269**, 1416 (1995).
- [14] P. Umari and A. Pasquarello, Phys. Rev. Lett. **95**, 137401 (2005).
- [15] E. D. Zanotto and D. R. Cassar, Sci. Rep. **7**, 43022 (2017).
- [16] D. R. Uhlmann, J. F. Hays, and D. Turnbull, Phys. Chem. Glasses **8**, 1 (1967).
- [17] A. Takada, C. R. A. Catlow, and G. D. Price, Phys. Chem. Glasses **44**, 147 (2003).
- [18] L. Huang, M. Durandurdu, and J. Kieffer, J. Phys. Chem. C **111**, 13712 (2007).
- [19] G. Ferlat, A. P. Seitsonen, M. Lazzeri, and F. Mauri, Nature Mat. **11**, 925 (2012).
- [20] F. Claeysens, J. N. Hart, N. C. Norman, and N. L. Allan, Adv. Funct. Mater. **23**, 5887 (2013).
- [21] M. Daub and H. Hillebrecht, Eur. J. Inorg. Chem. **2015**, 4176 (2015).
- [22] S. Sorella, M. Casula, and D. Rocca, J. Chem. Phys. **127**, 014105 (2007).
- [23] C. J. Umrigar, J. Toulouse, C. Filippi, S. Sorella, and R. G. Hennig, Phys. Rev. Lett. **98**, 110201 (2007).
- [24] M. Barborini, S. Sorella, and L. Guidoni, J. Chem. Theory Comput. **8**, 1260 (2012).
- [25] M. Casula, C. Filippi, and S. Sorella, Phys. Rev. Lett. **95**, 100201 (2005).
- [26] M. Casula, S. Moroni, S. Sorella, and C. Filippi, J. Chem. Phys. **132**, 154113 (2010).
- [27] M. Dagrada, S. Karakuzu, V. L. Vildosola, M. Casula, and S. Sorella, Phys. Rev. B **94**, 245108 (2016).
- [28] S. Sorella, *Turborvb, quantum monte carlo software for electronic structure calculations*, <http://people.sissa.it/~sorella/web/>.
- [29] See Supplemental Material at [] for computational details and additional data, which includes Refs. [].
- [30] D. C. Langreth and J. P. Perdew, Solid State Comm. **17**, 1425 (1975).
- [31] O. Gunnarsson and B. I. Lundqvist, Phys. Rev. B **13**, 4274 (1976).
- [32] A. Marini, P. García-González, and A. Rubio, Phys. Rev. Lett. **96**, 136404 (2006).

- [33] S. Lebègue, J. Harl, T. Gould, J. G. Ángyán, G. Kresse, and J. F. Dobson, *Phys. Rev. Lett.* **105**, 196401 (2010).
- [34] G. Kresse and J. Furthmüller, *Phys. Rev. B* **54**, 11169 (1996).
- [35] G. Kresse and D. Joubert, *Phys. Rev. B* **59**, 1758 (1999).
- [36] S. Grimme, *J. Comput. Chem.* **27**, 1787 (2006).
- [37] A. Tkatchenko and M. Scheffler, *Phys. Rev. Lett.* **102**, 073005 (2009).
- [38] K. Lee, E. D. Murray, L. Kong, B. I. Lundqvist, and D. C. Langreth, *Phys. Rev. B* **82**, 081101(R) (2010).
- [39] T. Thonhauser, S. Zuluaga, C. A. Arter, K. Berland, E. Schröder, and P. Hyldgaard, *Phys. Rev. Lett.* **115**, 136402 (2015).
- [40] J. P. Perdew, K. Burke, and M. Ernzerhof, *Phys. Rev. Lett.* **77**, 3865 (1996).
- [41] S. J. Clark, M. D. Segall, C. J. Pickard, P. J. Hasnip, M. J. Probert, K. Refson, and M. C. Payne, *Z. Kristallogr.* **220**, 567 (2005).
- [42] P. Giannozzi, S. Baroni, N. Bonini, M. Calandra, R. Car, C. Cavazzoni, D. Ceresoli, G. L. Chiarotti, M. Cococcioni, I. Dabo, et al., *J. Phys. Condens. Matter* **21**, 395502 (2009), URL <http://www.quantum-espresso.org>.
- [43] F.-X. Coudert, *Phys. Chem. Chem. Phys.* **15**, 16012 (2013).
- [44] H. Hay, Ph.D. thesis, Université Pierre & Marie Curie, Paris (2016), URL <https://tel.archives-ouvertes.fr/tel-0147013a1>.
- [45] P. Haas, F. Tran, and P. Blaha, *Phys. Rev. B* **79**, 085104 (2009).
- [46] H. Hay, G. Ferlat, M. Casula, A. P. Seitsonen, and F. Mauri, *Phys. Rev. B* **92**, 144111 (2015).
- [47] W. Sun, S. T. Dacek, S. P. Ong, G. Hautier, A. Jain, W. D. Richards, A. C. Gamst, K. A. Persson, and G. Ceder, *Sci. Adv.* **2**, e1600225 (2016).
- [48] The calculation of the mechanical moduli (Fig. 7) is readily available in the CRYSTAL14 code [59] for D2 only (among vdW schemes).
- [49] For binary oxides, the range of observed polymorphs (as defined by the 90th percentile of a statistical analysis [47]) is 94 meV/atom, i.e. 10.8 kcal/(mol B₂O₃). Taking silica as a close parent system, the highest energy above quartz (among SiO₂ polymorphs for which calorimetric data are available) is 6.88 kcal/(mol 2SiO₂) (ISV zeolite) [12].
- [50] M.-S. Wang, G.-C. Guo, W.-T. Chen, G. Xu, W.-W. Zhou, K.-J. Wu, and J.-S. Huang, *Angew. Chem. Int. Ed.* **46**, 3909 (2007).
- [51] M.-C. Liu, P. Zhou, H. G. Yao, S.-H. Ji, R.-C. Zhang, M. Ji, and Y.-L. An, *Eur. J. Inorg. Chem.* **31**, 4622 (2009).
- [52] N. E. Schmidt, *Russ. J. Inorg. Chem.* **11**, 241 (1966).
- [53] Minimal value of the Young modulus $E_{min} \geq 20$ GPa and elastic anisotropy $\eta \leq 5$, where η is $\max\left(\frac{E_{max}}{E_{min}}, \frac{G_{max}}{G_{min}}\right)$. However, the criterion on anisotropy likely does not apply to layered structures (T0, T0-0.5*b* and T0-*b*).
- [54] E. Perim, D. Lee, Y. Liu, C. Toher, P. Gong, Y. Li, W. N. Simmons, O. Levy, J. J. Vlassak, J. Schroers, et al., *Nat. Commun.* **7**, 12315 (2016).
- [55] C. H. L. Goodman, *Nature* **257**, 370 (1975).
- [56] G. G. Naumis, *Phys. Rev. E* **85**, 061505 (2012).
- [57] P. Ronceray and P. Harrowell, *Phys. Rev. E* **96**, 042602 (2017).
- [58] J. Russo, F. Romano, and H. Tanaka, *Phys. Rev. X* **8**, 021040 (2018).
- [59] R. Dovesi, R. Orlando, A. Erba, C. M. Zicovich-Wilson, B. Civalleri, S. Casassa, L. Maschio, M. Ferrabone, M. De La Pierre, P. D’Arco, et al., *Int. J. Quantum Chem.* **114**, 1287 (2014).